Received 1 March 2024; revised 10 April 2024; accepted 1 May 2024. Date of publication 6 May 2024; date of current version 22 May 2024.
The review of this article was arranged by Editor Z. Wang.

Digital Object Identifier 10.1109/JEDS.2024.3397014

Electrically Tunable Ideality Factor and Series Resistance of Gate-Controlled Graphene/Pentacene Schottky Junctions

TAE YOON LEE[1,2], YOON-JEONG KIM[1], SEOKHOON AHN[1,3], AND DAE-YOUNG JEON[4]

1 Institute of Advanced Composite Materials, Korea Institute of Science and Technology, Wanju 55324, Jeollabuk, Republic of Korea
2 Department of Physics Education, Seoul National University, Seoul 08826, Republic of Korea
3 Department of JBNU-KIST Industry-Academia Convergence Research, Jeonbuk National University, Jeonju 54896, Jeollabuk, Republic of Korea
4 Department of Electrical Engineering, Gyeongsang National University, Jinju 52828, Gyeongnam, Republic of Korea

CORRESPONDING AUTHORS: S. AHN AND D.-Y. JEON (e-mail: ahn75@kist.re.kr; dyjeon@gnu.ac.kr)

This work was supported in part by the Commercialization Promotion Agency for R&D Outcomes (COMPA) Grant funded by the Korean Government (Ministry of Science and ICT, 2023); in part by the National Research Foundation of Korea (NRF) under Grant 2022R1A6A3A01085928; in part by the Research Grant from Gyeongsang National University in 2023; and in part by the Regional Innovation Strategy (RIS) of the National Research Foundation of Korea (NRF) funded by the Ministry of Education (MOE) under Grant 2021RIS-003.

ABSTRACT Gate-tunable Schottky barrier diodes find many applications in logic transistors, photodiodes, and sensors. In this work, the electrical properties of Schottky barrier diodes with graphene/pentacene junctions and additional gates were investigated in detail. The results of modeling equations that considered the ideality factor, series resistance, and effective barrier-height according to the gate bias (V_g) were in good agreement with the experimental results. In addition, the dominant conduction mechanism when the effective barrier-height was controlled by V_g is discussed from the perspective of the temperature-dependent currents in Schottky barrier diodes. This work provides critical information that aids our understanding of gated Schottky diodes with graphene/pentacene junctions, increasing the possible practical applications thereof.

INDEX TERMS Gate-tunable Schottky barrier diodes, graphene/pentacene junction, ideality factor, series resistance, effective barrier-height, modeling.

I. INTRODUCTION

Organic semiconductors such as pentacene (with five benzene rings) are attractive in terms of electronic applications; they are inexpensive, easy to fabricate at low temperatures (T), and mechanically flexible [1], [2], [3]. Pentacene-based field-effect transistors, light-emitting diodes, photovoltaic devices, and advanced sensors have found applications in many fields such as display devices, flexible electronics, electronic papers and synaptic devices [4]. Graphene (a two-dimensional single-atomic layer material) has high mobility, good flexibility, and transparency, and it is compatible with the conventional top-down lithographic processes commonly used for fabrication of advanced electronic devices [4], [5], [6]. The junction between the organic semiconductor and the graphene electrode creates a Schottky contact that can serve as a valuable building block when creating novel hybrid devices [7], [8], [9], [10]. Notably, the Schottky barrier at an organic semiconductor/graphene interface can be modulated via gate voltage control of the work functions of both the organic semiconductor and graphene. This is why a gate-controlled Schottky barrier with a graphene electrode is also termed a barristor [11]. A few studies have explored the electrical properties of gated Schottky diodes based on organic semiconductors and graphene [7], [8], [9], [10], [12]. However, further electrical characterization by considering equivalent circuit models and derivation of important parameters such as barrier height, ideality factor and series resistance, for Schottky diodes tuned by gates remains to be achieved.

In this paper, Schottky barrier diodes based on graphene/pentacene junctions were fabricated with additional gate electrodes and subjected to T-dependent measurements. Then, the electrical properties were investigated in detail with a focus on the ideality factor, series resistance (R_s),

© 2024 The Authors. This work is licensed under a Creative Commons Attribution 4.0 License.
For more information, see https://creativecommons.org/licenses/by/4.0/

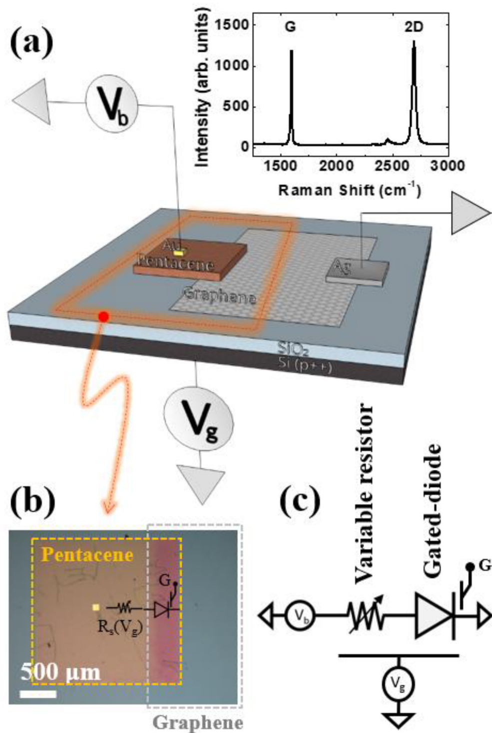

FIGURE 1. (a) Schematic of a graphene/pentacene Schottky junction controlled by V_g; the inset shows the Raman spectrum of graphene. (b) Optical microscopy image of the fabricated pentacene/graphene heterojunction. (c) Equivalent circuit model of gated Schottky diodes based on graphene/pentacene. The variable resistor is a series resistance that changes as the resistance of pentacene and graphene vary according to V_g.

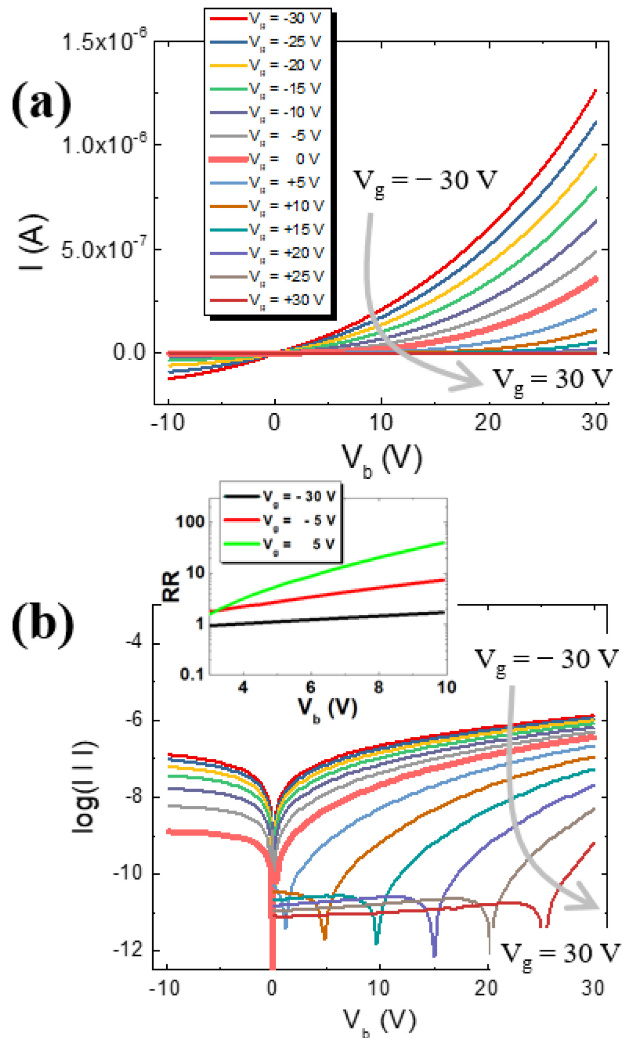

FIGURE 2. Current (I) versus the bias voltage (V_b) curve of a graphene/pentacene Schottky diode at various V_g values from −30 V to +30 V, at room temperature on a (a) linear and (b) a logarithmic scale. The inset of Fig. 2(b) shows RR depending on V_g.

and effective barrier-height, all of which were extracted from modeling equations.

II. EXPERIMENTS

Graphene was synthesized on a Cu foil using a conventional chemical vapor-deposition growth method in a mixture of CH_4 and H_2. Polymethyl methacrylate (PMMA) was coated onto the synthesized graphene, and the PMMA film/graphene structure was then suspended by etching the Cu foil using an ammonium persulfate solution. Finally, graphene was transferred to a 300-nm-thick SiO_2/highly doped-Si substrate [13]. Raman spectroscopy at 514 nm identified the grown graphene. The electrical characteristics were measured with an HP4156A semiconductor parameter analyzer in the T range of 100–300 K.

The inset of Figure 1(a) shows the Raman spectrum of graphene; the two typical principal peaks are the G peak (attributable to the primary in-plane vibrational mode at 1,580 cm^{-1}) and the 2D peak (a second-order overtone of a different in-plane vibration D mode at 2,690 cm^{-1}) [14]. A pentacene film 100 nm in thickness was thermally evaporated onto graphene at ≈ 0.3 Å/s followed by evaporation of Au using a shadow mask to form the electrodes.

Figure 1(a) and 1(b) show a schematic and an optical microscopy (OM) image of a device with a graphene/pentacene Schottky junction. In the OM image, the color gradient of the pentacene layer reveals the extent of the graphene layer under pentacene. The pentacene layer on the right, which is rather dark in color, is a pentacene/graphene heterostructure. Figure 1(c) is the equivalent circuit diagram of the fabricated graphene/pentacene device. The electrical properties of a Schottky diode with a pentacene/graphene heterojunction can be changed by varying the global back-gate voltage (V_g), which gates the Schottky diodes. The resistance of both pentacene and graphene can be changed by varying the V_g value (i.e., the variable resistor is tuned using V_g) because the Fermi levels of pentacene and the work function of graphene are dependent on the electric field (E-field) associated with V_g [11], [12].

III. RESULTS AND DISCUSSION

The current through the graphene/pentacene junction was strongly modulated by the gate voltage. Figure 2(a) and 2(b) show the current (I) versus the bias voltage (V_b) curves of

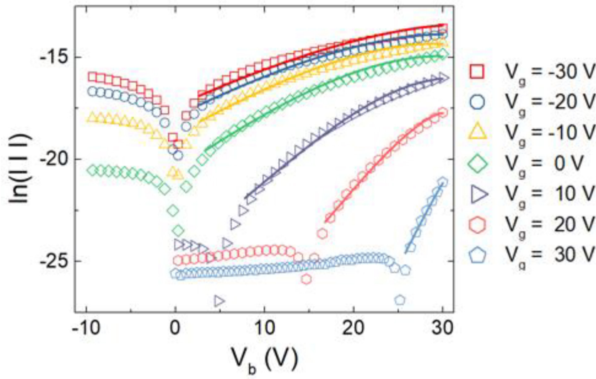

FIGURE 3. I versus V_b curves as V_g varies (natural logarithmic scale). The measured values (symbols) were well-fitted by the solid line derived using the Schottky diode equation that considered R_s and V_{offset}.

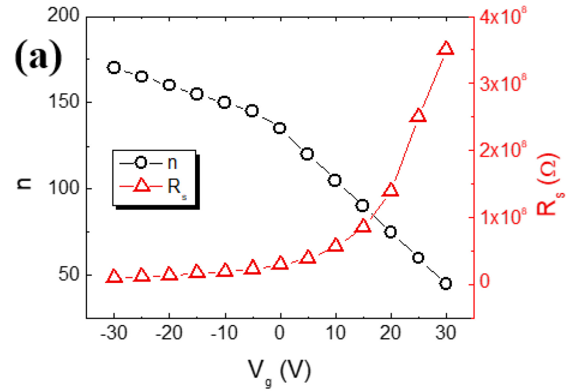

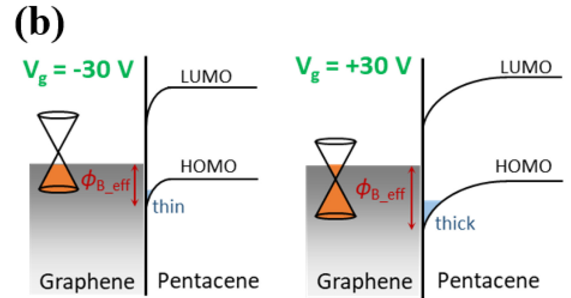

FIGURE 4. (a) V_g dependence of the extracted n and R_s values. (b) Energy band diagrams of graphene/pentacene heterojunctions under negative (left) and positive V_g (right) V_g. HOMO and LUMO mean the highest occupied molecular orbital and lowest unoccupied molecular orbital, respectively.

the graphene/pentacene Schottky diode at room T on linear and logarithmic scales, respectively. The I–V_b curve data were derived as V_g varied from −30 V to +30 V. The curves clearly reveal typical diode-like electrical characteristics. The current flow was larger under a positive V_b than under a negative V_b at a negative V_g. On the other hand, as V_g increased, the turn-on voltage in the positive direction rose. In addition, an increase in V_g improved rectification, thus reducing the leakage current and enhancing current acceleration as V_b varied. Such enhanced rectification may reflect the status of the Schottky barrier, the effectiveness of which is controlled by V_g. Indeed, the extracted rectification ratio [RR (V_b, V_g) = I (V_b)/I(−V_b) at V_g] in the inset of Fig. 2(b) was noticeably improved as increasing V_g [15].

Figure 3 shows the I–V_b curves obtained at room T using a natural logarithmic scale. To investigate the V_g-dependent characteristics of currents in the graphene/pentacene junction, we extracted the relevant parameters using the Schottky diode equation [16]:

$$I = I_s \times \left(e^{\frac{qV_D}{n \cdot kT}} - 1\right) \tag{1}$$

where V_D is the voltage drop across the graphene/pentacene junction; and I_s, q, n, k, and T are the reverse bias saturation current, elementary charge, ideality factor, Boltzmann constant, and absolute T, respectively. When the effects of R_s and offset bias (V_{offset}) are taken into account, V_D can be expressed in terms of V_b. V_{offset} is closely related to a turn-on voltage of Schottky barrier diodes. Before reaching the V_{offset}, there were no significant current flows. Thus, V_D = V_b − I·R_s + V_{offset}; and, for V_D > n·kT/q, Equation (1) can be rewritten as [17]:

$$I \approx I_s(V_g) \times e^{\left(\frac{q\left[V_b - I \cdot R_s(V_g) + V_{offset}(V_g)\right]}{n(V_g) \cdot kT}\right)} \tag{2}$$

where R_s mainly reflects the pentacene and graphene self-resistance. As the concentration of mobile charge carriers in pentacene and the work function of graphene are affected by V_g, the resistance of both pentacene and graphene is dependent on V_g [18], [19], [20], [21]. Therefore, R_s is V_g-dependent. V_{offset} is affected by the value of the Schottky barrier and the interface states at heterojunctions. Therefore, V_{offset} is also V_g-dependent. Equation (2) was used to fit data when investigating the diode properties of the gated Schottky barrier device. Indeed, as can be seen in the measured data of Figure 3 (marked with symbols), both I_s and V_{offset} depended on V_g. Fitting revealed that the ideality factor and R_s were also influenced by V_g. These effects of V_g on a gated Schottky barrier device can change the dominant transport mechanism, as will be discussed below.

The gated Schottky barrier device based on graphene/pentacene exhibited near-ideal Schottky diode characteristics under a positive V_g but not a negative V_g. As discussed above, n, R_s, and I_s were extracted via fitting of the Schottky barrier diode equation (Eq. (2)) to the experimental values. Figure 4(a) shows the V_g dependence of the extracted n and R_s. The ideality factor decreased as V_g increased. In our device, n decreased from 170 to 45 as V_g increased from −30 V to +30 V. A large ideality factor (n) could be due to tunneling based Schottky-barrier lowering mechanism such as field-emission and thermionic field-emission. In addition, the presence of interfacial layer and interface state might result in the value of n [16], [22], [23]. However, R_s rose as V_g increased. The changes in n and R_s were more dramatic under positive V_g than negative V_g. The effect of V_g on the Schottky barrier should be further investigated to determine the causes of such parameter changes. Figure 4(b) shows

band diagrams of a graphene/pentacene heterojunction under a negative and positive V_g, respectively. It is known that the Fermi level of graphene can be modulated by an external E-field [18]. As is apparent in Figure 4(b), a negative V_g is associated with hole-rich graphene; the effective Schottky barrier height (Φ_{B_eff}) then falls. In contrast, a positive V_g increases Φ_{B_eff} and thus induces large shifts in the Schottky diode threshold voltages. Moreover, V_g affects both the barrier width and Φ_{B_eff} [19]. A graphene layer does not perfectly screen the E-field given the low density of states near the Dirac point and the fact that the layer is ultra-thin [20]. Given this imperfect E-field screening, pentacene can be electrically doped by the E-field of V_g at the graphene/pentacene interface. As a result, the barrier width can also be modulated by V_g. As pentacene is a p-type semiconductor, it becomes relatively more electrically doped under a negative compared to a positive V_g. As the hole doping concentration increases, the effective width of the Schottky barrier narrows [16], [21]. As shown in Figure 4(b), the barrier width becomes narrower under a negative compared to a positive V_g. The narrow barrier induced by a negative V_g enhances the contribution of field emission to electrical transport at the graphene/pentacene junction. However, under a positive V_g, the barrier is too wide to allow active field emission. Therefore, when the Schottky barrier is wide under a positive V_g, thermionic emissions may dominate the transport mechanism.

To further investigate the effect of V_g on the graphene/pentacene interface, the experiments were repeated at different T from 150 to 300 K at intervals of 25 K. Figure 5(a) and 5(b) show plots of the diode currents with different V_g, respectively. The current level fell noticeably as T decreased. In other words, at lower T, a larger V_g or V_b magnitude is required to attain the same current level. Under such conditions, simple thermionic emission explains a large proportion of transport across the graphene/pentacene junction [16]. The diode current at 300 K is about one order of magnitude larger than the current at 150 K for $V_g = -30$ V. On the other hand, at $V_g = +30$ V, the current at 300 K is about two orders of magnitude greater than that at 150 K. Also, at $V_g = +30$ V, the threshold voltage increases significantly as T decreases. The different T dependencies show that field emission becomes more dominant, and then complete, at $V_g = -30$ V. The differences in the transport mechanisms can be explained by increases in the effective height and width of the Schottky barrier at a positive V_g, as shown in Figure 4(b). Figure 5(c) show Arrhenius plots for different V_g values at a forward V_b. A clear linear dependency is apparent, which means that thermionic emission is the dominant transport mechanism [24]:

$$I = A \cdot A^* \cdot T^2 \cdot e^{\left(-\frac{\Phi_{eff} - qV_b}{kT}\right)} \tag{3}$$

where A is the junction area, A* is the effective Richardson constant, and Φ_{eff} is the effective Schottky barrier height modulated by V_g.

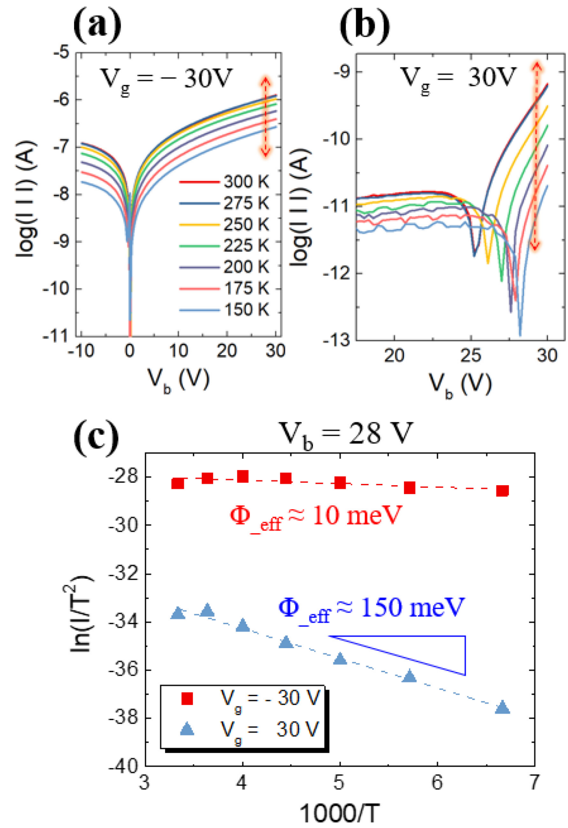

FIGURE 5. Schottky diode currents at varying temperatures for (a) $V_g = -30$ V and (b) $V_g = 30$V. (c) Arrhenius plots drawn at different V_g values to allow extraction of Φ_{eff}.

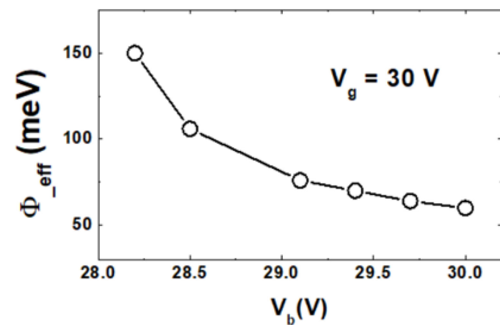

FIGURE 6. Φ_{eff} as a function of V_b, extracted by the Arrhenius plots at $V_g = 30$ V.

At a $V_g = +30$ V, the Φ_{eff} was about 150 meV, similar to the value reported in a previous study [12]. As V_g decreased, Φ_{eff} fell; Φ_{eff} was about 10 meV at $V_g = -30$ V. The very small Φ_{eff} at $V_g = -30$ V may be attributable to the reductions in Schottky barrier height and width shown in Figure 4(b). At $V_g = -30$ V, a small and narrow Schottky barrier could eventually render field emission dominant. As a result, at $V_g = -30$ V, the graphene/pentacene junction changes from a Schottky contact to an ohmic-like contact, and the device exhibits poor diode characteristics and thus the large ideality factor shown in Figure 4(a).

Φ_{eff} versus V_b was also extracted in Figure 6. Indeed, Φ_{eff} was decreased as increasing V_b at $V_g = 30$ V, while

there were no significant changes on the Φ_{eff} with varying V_b at $V_g = -30$ V.

IV. CONCLUSION

In summary, we fabricated gated Schottky barrier diodes with graphene/pentacene heterojunctions and investigated the dominant transport mechanisms at various V_g and T values. The graphene/pentacene junction created a Schottky contact, and various properties, including the height and width of the Schottky barrier, were modulated by V_g after adjusting the Fermi level of pentacene and the work function of graphene. The thermionic effect was dominant during electrical transport by the device under a positive V_g. However, under a negative V_g, field emission became dominant. Thus, the transport mechanism of a graphene/pentacene Schottky diode changed dramatically as V_g varied. When the magnitude of negative V_g increased, the heterojunction exhibited electrical properties that were close to ohmic in nature. On the other hand, as the magnitude of positive V_g increased, typical Schottky diode characteristics developed. Our results provide useful insights into the transport mechanisms within gate-tunable Schottky diodes featuring graphene/pentacene heterojunctions.

REFERENCES

[1] A. Facchetti, "Semiconductors for organic transistors," *Mater. Today*, vol. 10, no. 3, pp. 28–37, 2007, doi: 10.1016/S1369-7021(07)70017-2.
[2] Y.-Y. Lin, D. J. Gundlach, S. F. Nelson, and T. N. Jackson, "Stacked pentacene layer organic thin-film transistors with improved characteristics," *IEEE Electron Device Lett.*, vol. 18, no. 12, pp. 606–608, Dec. 1997, doi: 10.1109/55.644085.
[3] H. Klauk, D. J. Gundlach, J. A. Nichols, and T. N. Jackson, "Pentacene organic thin-film transistors for circuit and display applications," *IEEE Trans. Electron Devices*, vol. 46, no. 6, pp. 1258–1263, Jun. 1999, doi: 10.1109/16.766895.
[4] B. S. Bhardwaj et al., "Orientation analysis of pentacene molecules in organic field-effect transistor devices using polarization-dependent Raman spectroscopy," *Sci. Rep.*, vol. 9, no. 1, 2019, Art. no. 15149, doi: 10.1038/s41598-019-51647-2.
[5] M. J. Allen, V. C. Tung, and R. B. Kaner, "Honeycomb carbon: A review of graphene," *Chem. Rev.*, vol. 110, no. 1, pp. 132–145, 2010, doi: 10.1021/cr900070d.
[6] K. S. Novoselov, V. I. Fal'ko, L. Colombo, P. R. Gellert, M. G. Schwab, and K. Kim, "A roadmap for graphene," *Nature*, vol. 490, no. 7419, pp. 192–200, 2012, doi: 10.1038/nature11458.
[7] K. Berke, S. Tongay, M. McCarthy, A. Rinzler, B. Appleton, and A. Hebard, "Current transport across the pentacene," *J. Phys. Condens. Matter*, vol. 24, no. 25, 2012, Art. no. 255802, doi: 10.1088/0953-8984/24/25/255802.
[8] W.-T. Hwang et al., "Gate-dependent asymmetric transport characteristics in pentacene barristors with graphene electrodes," *Nanotechnology*, vol. 27, no. 47, 2016, Art. no. 475201, doi: 10.1088/0957-4484/27/47/475201.
[9] G. Oh et al., "Graphene/pentacene barristor with ion-gel gate dielectric: flexible ambipolar transistor with high mobility and on/off ratio," *ACS Nano*, vol. 9, no. 7, pp. 7515–7522, 2015, doi: 10.1021/acsnano.5b02616.
[10] M. D. Mansour et al., "Nanoscale electronic transport at graphene/pentacene van der Waals interfaces," *Nanoscale*, vol. 15, no. 20, pp. 9203–9213, 2023, doi: 10.1039/D2NR06682C.
[11] H. Yang et al., "Graphene barristor, a triode device with a gate-controlled Schottky barrier," *Science*, vol. 336, no. 6085, pp. 1140–1143, 2012, doi: 10.1126/science.1220527.
[12] C. Ojeda-Aristizabal, W. Bao, and M. Fuhrer, "Thin-film barristor: A gate-tunable vertical graphene-pentacene device," *Phys. Rev. B*, vol. 88, no. 3, 2013, Art. no. 35435, doi: 10.1103/PhysRevB.88.035435.
[13] D. H. Shin, Y.-J. Kim, S.-K. Lee, S. Bae, and S. Ahn, "Atomically thin alkane passivation layer for flexible and transparent graphene electronics," *Appl. Surface Sci.*, vol. 612, Mar. 2023, Art. no. 155695, doi: 10.1016/j.apsusc.2022.155695.
[14] J.-B. Wu, M.-L. Lin, X. Cong, H.-N. Liu, and P.-H. Tan, "Raman spectroscopy of graphene-based materials and its applications in related devices," *Chem. Soc. Rev.*, vol. 47, no. 5, pp. 1822–1873, 2018, doi: 10.1039/C6CS00915H.
[15] S. Sherif, G. Rubio-Bollinger, E. Pinilla-Cienfuegos, E. Coronado, J. C. Cuevas, and N. Agraït, "Current rectification in a single molecule diode: The role of electrode coupling," *Nanotechnology*, vol. 26, no. 29, 2015, Art. no. 291001, doi: 10.1088/0957-4484/26/29/291001.
[16] S. M. Sze, Y. Li, and K. K. Ng, *Physics of Semiconductor Devices*. Hoboken, NJ, USA: Wiley, 2021, doi: 10.1002/0470068329.
[17] C. Yim, N. McEvoy, E. Rezvani, S. Kumar, and G. S. Duesberg, "Carbon–silicon Schottky barrier diodes," *Small*, vol. 8, no. 9, pp. 1360–1364, 2012, doi: 10.1002/smll.201101996.
[18] A. K. Geim and K. S. Novoselov, "The rise of graphene," *Nat. Mater.*, vol. 6, no. 3, pp. 183–191, 2007, doi: 10.1038/nmat1849.
[19] A. Di Bartolomeo, "Graphene Schottky diodes: An experimental review of the rectifying graphene/semiconductor heterojunction," *Phys. Rep.*, vol. 606, pp. 1–58, Jan. 2016, doi: 10.1016/j.physrep.2015.10.003.
[20] N. Lee et al., "The interlayer screening effect of graphene sheets investigated by Kelvin probe force microscopy," *Appl. Phys. Lett.*, vol. 95, no. 22, 2009, Art. no. 222107, doi: 10.1063/1.3269597.
[21] S. Cristoloveanu, K. H. Lee, H. Park, and M. S. Parihar, "The concept of electrostatic doping and related devices," *Solid-State Electron.*, vol. 155, pp. 32–43, May 2019, doi: 10.1016/j.sse.2019.03.017.
[22] E. H. Rhoderick and R. H. Williams, *Metal-Semiconductor Contacts*. Oxford, U.K.: Clarendon Press, 1988, doi: 10.1049/ip-i-1.1982.0001.
[23] F. Yakuphanoglu, "Electrical characterization and interface state density properties of the ITO/C70/Au Schottky diode," *J. Phys. Chem. C*, vol. 111, no. 3, pp. 1505–1507, 2007, doi: 10.1021/jp066912q.
[24] K. Chino, "Behavior of Al-Si Schottky barrier diodes under heat treatment," *Solid-State Electron.*, vol. 16, no. 1, pp. 119–121, 1973, doi: 10.1016/0038-1101(73)90132-9.